RSC Advances

ROYAL SOCIETY OF CHEMISTRY

www.rsc.org/advances

Modeling the relationship between melting point of the metal nanowire and its cap surface curvature

Y. Jiang[1], K.Zhang[2,3,*]

[1] *Centre for Advanced Macromolecular Design, School of Chemical Engineering, University of New South Wales UNSW, Kensington NSW 2052, Australia*

[2] *Key Laboratory of Microgravity (National Microgravity Laboratory), Institute of Mechanics, Chinese Academy of Sciences, Beijing 100190, China*

[3] *National Engineering Research Central for Rare Earth Materials, General Research Institute for Non-Ferrous Metals, GRIREM Advanced Co. Ltd., Beijing100088, China*

Email: *zhangkunone@gmail.com*

Keywords*:* molecular dynamics simulations, nanoconfinement, embedded particle, surface curvature, melting point

Abstract

It is of practical importance to predict the melting point of metal nanowires in confined environment. Based on molecular dynamics (MD) simulations, a universal model unraveling the relationship between the melting point of the metal nanowire in nanoconfinement and its cap surface curvature has been developed for the first time. The results have demonstrated that both the interaction strength between the nanowire and the nanoconfinement and the diameter of nanoconfinement dramatically affect the melting point of the embedded nanowire. These phenomena can be further deduced into a mathematical formula directly describing the curvature-dependent melting point. It is also found that the melting feature of the metal nanowire under weak interaction is quite different from that under strong interaction. Furthermore, the melting point of the free

cluster can also be predicted using this model. Our findings have provided a direct way to analyze the melting point *via* the observed morphology of the metal nanoparticle.

Introduction

Metal nanoparticles, including free or substrate-supported clusters and nanowires in nanoconfinement, are currently used or have potential applications in catalytic, optical, magnetic, electronic, and alternative energy fields due to the particular lower-dimensional advantages and the nanoscale structures.[1,2] Especially, as for the nanowire in nanoconfinement, the nanoconfinement such as carbon nanotubes, not only acts as natural protection of the embedded nanowires against oxidation, [3] but also gives the embedded nanowires more desirable properties, which makes the embedded nanowires more stable and durable for these applications.[4] For example, melting point shift caused by the nanoconfinement tends to be a critical issue in practice because it may alter the features of the solid-state particle. In terms of the free or substrate-supported cluster, it has been well recognized that the melting temperature has a depressive tendency which yields the same linear or approximately linear equation with the reciprocal of the cluster diameter:[5-8]

$$\Delta T = T_m - T_n = \frac{\beta}{D} T_m \qquad (1)$$

Where T_n and T_m are the melting points of the cluster and the bulk, respectively, and β is a model-related parameter. Moreover, several models have been developed to explain the depression of the melting point, including the homogeneous melting model,[9] the liquid skin melting model [10] and the liquid nucleation and growth model [11,12] on the basis of different melting mechanisms.

Meanwhile, Jackson and McKenna investigated the glass transition shift of organic liquids confined in pores, which has stimulated more and more people to research the phase transition happened in porous media. [13] The fundamental interest in this realm is to

understand the influence that the nanoconfinement brings to the phase transition, from phenomena to mechanism.[14] The melting point shift becomes particularly essential for the fabrication of nanomaterials in porous templates, which may be of great significance for catalysts, semiconductor device, nonmagnetic recording media, fuel cell and etc.[15-18] According to the existing experimental evidence on the embedded metals in porous media, enormous works refer to the observation that the melting temperature depression is also inversely proportional to the pore size. [19,20] In addition, for the embedded nanowires, it is also found that the melting behavior is controlled not only by the particle size but also by the particle/matrix interfaces.[21] The melting point depression of embedded nanowires, *ΔT,* as elucidated by the Gibbs-Thomson equation, an accepted thermodynamic model, is given by: [22,23]

$$\Delta T = T_m - T_n = T_m \frac{4\sigma_{sl}}{\Delta H_f \rho_s D} \qquad (2)$$

where σ_{sl} is the surface energy at the liquid-solid interface of the embedded material, T_m is the bulk melting point, T_n is the melting point of the embedded metal, D is the diameter of the tubular confinement, ΔH_f is the bulk enthalpy of fusion, and ρ_s is the density of the solid. Although this thermodynamic relationship has been conventionally employed to describe the lowering melting point of the embedded metal nanowires, there still exist ultimate limitations due to several improper assumptions. The most dominant one is that the interaction between the embedded particle and confinement has been omitted. Actually, the universality and practicality of the equation has already been challenged by some superheating phenomena of the embedded substances in porous system. [24,25] The existed model is not all-inclusive and the comprehensive theory is of great need.

In our studies, MD simulations on the embedded metal nanowire in nanoconfinement has been carried out in a wide range of interaction strength and confinement size to investigate the relationship between T_m and the nanoconfinement and to answer whether the negative ΔT is possible. As existed in bulk metal material,[26] another universal model accounting for the relation between the melting point and the surface curvature of the embedded metal nanowires has been proposed for the sake of the physical analysis and the manipulation on the melting point of the embedded nanowires. The melting mechanisms at the different interaction strength have also been illustrated in details to provide insights to the interaction between the metal atoms and the nanoconfinement.

Details of Methods

Herein, Fe nanowire has been chosen as the embedded particle, and porous systems such as carbon nanotubes and nanoscale pores have been abstracted into a tubular confinement with variable diameter and interaction strength.

The second-moment approximation of the tight-binding (TB-SMA) potential was employed to describe the Fe-Fe interactions.[27] The TB-SMA potential parameters for Fe-Fe were presented elsewhere.[28] A Lennard-Jones 9/3 potential was used to describe the interaction between the Fe atoms and the confinement:

$$V(z) = \varepsilon \frac{3\sqrt{3}}{2}\left[\left(\frac{\sigma}{z}\right)^9 - \left(\frac{\sigma}{z}\right)^3\right] \qquad (3)$$

The parameter σ was kept constant at 0.2 nm, and the depth of potential well ε which dominates the confinement-metal interaction strength ranges from 0.1 to 0.8 eV to adjust the surface curvature of the embedded particle.

The structure evolution of Fe_N in the melting process was studied by constant temperature MD using the Berendsen method and an integration time step of 3fs.[29] The

initial structures for the melting process were obtained by relaxing and annealing the randomly embedded nanowire at 500 K to reach the equilibration. In the melting process, the initial structures were heated from 800 K to 1600 K with a temperature ramp of 10 K and 500,000 MD steps at each constant temperature point.

In addition, it has been tested that when the length-to-diameter ratio of the embedded particle is larger than 2.5, the melting point of the particle becomes independent on its length. (**Figure S1**) Therefore, the length-to-diameter ratio of all the samples in this study was set to be 3. The simulated melting point of bulk iron was obtained by extrapolating the cluster melting point to infinitely large size. The bulk Fe melting point we obtained is lower than the reported value. The difference between the simulated value and experiment one may be caused by the inclusion of free cluster surfaces in the simulations or inaccuracies in the force field.[30] This difference, which is attributed to the calculation methods we employed, does not affect the conclusions reported here because the current research mainly focuses on the melting point shift law of the embedded nanowires.

Results and discussion

The main focus of the current work is to explore what influence the nanoconfinement exerts on the melting point of the embedded metal nanowires. **Figure 1a** shows the morphology of Fe_{4800} nanowires in tubular nano confinements. The diameter of the confinement was set to be 32 Å. With the increase of confinement-metal interaction by increasing the potential parameter ε from 0.1 eV to 0.8 eV, the surface curvature of the Fe_{4800} gradually decreased and the morphology exhibited three typical cases ranging from convex to concave (**Figure S2**). This indicated a valid effect of potential parameter on the surface curvature, which changed the accuracy of the above mentioned Gibbs-Thomson equation where the embedded particle was generally considered to be crystal with convex surface in the confinement. As for the corresponding energy curves in **Figure 1b**, where the

saltation point in each total energy curve was identified as the melting point at the given interaction strength. It is evident that the melting point increases with the enhanced interaction when Fe_{4800} was embedded in the confinement with the constant diameter; so that the potential parameter ε should not be ignored in the Gibbs-Thomson equation. Furthermore, it was clearly seen that for the nanowires embedded in the nanoscale confinement, the melting point could be higher, lower than or even equal to the bulk value (1370 K), which depended on the interaction strength between the confinement and the embedded particle. Therefore, the negative ΔT is possible when the interaction between the particle and the confinement is strong enough, which is also in agreement with the previous work reported by K. K. Nanda *et al*.[31]

As reported by Hu and his coworkers [32-34], the size and geometry have a significant effect on the melting point of the nanoparticles with the appearing of the quasi-liquid phase. Actually, the nanoconfinement can affect the dimension of the embedded particles and at the same time it also introduces the size-dependent effect to the particles.[35] As the size of the particle decreases towards the atomic scale, the melting point will also shift with the particle size changing. In **Figure 2a and 2b**, we investigated the size effect on the surface curvature and the melting point, respectively. To ensure the proper length-to-diameter ratio, the Fe nanowires were built with diameters of 16, 20, 24, 28 and 32 Å, consisting of 400, 900, 1800, 3100, 4800 atoms, respectively. Results demonstrated that the melting points of the embedded Fe nanowires tended to increase, while the surface curvature had a decreasing tendency as the diameter increase. These phenomena provided more proofs that the diameter had great effects on the phase transition process. The inset in **Figure 2b** also showed the melting point difference ΔT between the maximum potential parameter ε = 0.8 eV and the minimum potential parameter ε = 0.1 eV as a function of the diameter. The decreasing tendency of ΔT against diameter indicated that the size effect was receding with

the increasing diameter. According to the results in **Figure 1**, the effect of interaction strength ε should be added in the relationship defined by Eq. (2) besides the diameter D. Herein, considering that the surface curvature, similar to the melting point, is the combined results of the interaction strength ε and the diameter D. It is evident that the melting point is strongly correlated to the surface curvature which can be easily measured under the electron microscopy. We employed the surface curvature k as a single parameter to replace the parameters ε and D in the melting point variation equation, which can be described by the following expression:

$$T_n = (1 - \alpha k) T_m \qquad (4)$$

where T_m is the free bulk melting point, T_n is the melting point of the embedded metal particle, α is a material-dependent constant standing for all the material parameters mentioned in the Gibbs-Thomson equation which depend on the properties of the embedded material, and k is the surface curvature. This equation represents a linear correlation between the melting point and the surface curvature. To confirm the validity of Eq. (4), the graph in **Figure 2c** plots the melting points as a function of the surface curvatures, which fits well to the law in Equation (4). A negative curvature indicates an increased melting temperature, whereas a positive curvature means that the melting point of the embedded particle is lower than that of the bulk one. The slope of the line fixed by the melting points is the value of α. The simulation results and Equation (4) make us reconsider the conditions used in the Gibbs-Thomson equation and think about why it cannot fit the experimental results well. This relationship is in good agreement with the substantial experimental and theoretical results that have already been reported.[22] Based on this relationship, we can also predict and even control the melting point of the embedded nanowires in nanoconfinement.

In order to further investigate the influence of surface curvature on melting

mechanisms, the Lindemann index [8] at each time step was calculated. **Figure 3** shows the Lindemann indices of the embedded Fe_{1800} at ε = 0.1eV and 0.8 eV and the morphology of the embedded nanowires at the corresponding temperature. As shown in **Figure 3a**, at ε = 0.1eV the particle represents a convex surface and the surface atoms seem to diffuse more easily than the inner ones at T = 1040 K due to their poor coordination and weaker constraints. This leads to the formation of liquid-like capes when the temperature ramps to 1180 K and then the whole particle melts quickly at the melting point of 1200 K. This melting pattern is defined as the cape-induced melting. In contrast to the melting model under the weak interaction, the confinement exerts a strong constraint on the embedded particle at ε = 0.8 eV (in **Figure 3b**). The surface curvature is negative. The atoms close to the confinement are less mobile than those at ε = 0.1eV because they are almost fixed by the strong interaction between the confinement and the Fe atoms. Therefore, when the lowest point of the concave surface starts melting at 1300 K, the phase transformation occurs along the length in the inner layer where the constraint from the confinement is weaker than the outer layers. With the temperature rising, the melting of embedded particle slowly defuses from the inside out and completes at 1460 K. And this melting pattern is identified as the inner-diffusing melting. Therefore, with the increase of the interaction strength, the melting mechanism of embedded nanowires gradually evolves from the cape-induced melting to the inner-diffusing melting, which cannot be reduced into a single pattern as reported in the previous works.[19]

It has been confirmed that the melting point of free cluster follow the expression in Equation (1). Interestingly, Equation (1) can also be summarized into Equation (4) by replacing $1/D$ with k. This indicates that the melting point of the free clusters also follows the universal relation described in Equation (4). MD simulations have been further conducted to obtain the melting points of the free clusters between N = 400 and N = 7000,

and the results yield the established relationship as well (in **Figure 4**). On the aspect of relation, Equation (1) and (4) are the same in nature. Therefore, it can be generalized that the surface curvature is of universal significance to the prediction of the cluster melting temperature.

Conclusion

Systematic analyses have shed light on the curvature-dependent melting point of metal nanowires in the nanoconfinement. We have summarized this relationship into a linear model between the surface curvature k and the melting point T_n of the embedded metal nanowire: $T_n = (1-\alpha k)T_m$, where α is a material constant and T_m is the corresponding melting point of the metal in bulk. This equation is important to predict, measure, and even control the melting point of the metal nanoparticle in experiment and application. The model elucidates that the melting point of the metal nanowires embedded in the nanoscale porous media would be lower or higher than or equal to their bulk counterparts. Based on our simulations, the melting mechanism of the embedded nanowires can be sorted into the cap-induced melting and the inner-diffusing melting with the variation of the interaction strength. As an extension, this model is also applicable for the prediction of the melting point of the free metal cluster. Our findings would pave way to the application of the metal nanowires confined in porous media at different temperature range.

Acknowledgement

The authors would like to acknowledge the support by the National Natural Science Foundation of China (Grant Nos. 51401028). We also thank Shanghai Supercomputer Center for computational support.

References

[1] W. Liu, T.-z. Yang, G. Chu, J.-s. Luo, and Y.-j. Tang, Transactions of Nonferrous Metals Society of China **17**, 1347 (2007).

[2] C. Q. Sun, Progress in Solid State Chemistry **35**, 1 (2007).

[3] P. R. Couchman and W. A. Jesser, Nature **269**, 481 (1977).
[4] R. Shi, J. Shao, X. Zhu, and X. Lu, The Journal of Physical Chemistry C **115**, 2961 (2011).
[5] L. Gråbaek, J. Bohr, E. Johnson, A. Johansen, L. Sarholt-Kristensen, and H. H. Andersen, Physical Review Letters **64**, 934 (1990).
[6] W. Y. Choi, J. W. Kang, and H. J. Hwang, Physical Review B **68**, 193405 (2003).
[7] W. Qi, Y. Li, S. Xiong, and S.-T. Lee, Small **6**, 1996 (2010).
[8] F. Ding, A. Rosén, S. Curtarolo, and K. Bolton, Applied Physics Letters **88** (2006).
[9] M. Zhang, M. Y. Efremov, F. Schiettekatte, E. A. Olson, A. T. Kwan, S. L. Lai, T. Wisleder, J. E. Greene, and L. H. Allen, Physical Review B **62**, 10548 (2000).
[10] M. Dippel, A. Maier, V. Gimple, H. Wider, W. E. Evenson, R. L. Rasera, and G. Schatz, Physical Review Letters **87**, 095505 (2001).
[11] K. F. Peters, Y.-W. Chung, and J. B. Cohen, Applied Physics Letters **71**, 2391 (1997).
[12] K. F. Peters, J. B. Cohen, and Y.-W. Chung, Physical Review B **57**, 13430 (1998).
[13] C. L. Jackson and G. B. McKenna, Journal of Non-Crystalline Solids **131–133, Part 1**, 221 (1991).
[14] C. Alba-Simionesco, B. Coasne, G. Dosseh, G. Dudziak, K. E. Gubbins, R. Radhakrishnan, and M. Sliwinska-Bartkowiak, J Phys-Condens Mat **18**, R15 (2006).
[15] W. D. Zhang, Y. Wen, S. Min Liu, W. C. Tjiu, G. Qin Xu, and L. Ming Gan, Carbon **40**, 1981 (2002).
[16] S. Arcidiacono, J. H. Walther, D. Poulikakos, D. Passerone, and P. Koumoutsakos, Physical Review Letters **94**, 105502 (2005).
[17] Y. Kondo and K. Takayanagi, Science **289**, 606 (2000).
[18] A. Titov, P. Zapol, P. Král, D.-J. Liu, H. Iddir, K. Baishya, and L. A. Curtiss, The Journal of Physical Chemistry C **113**, 21629 (2009).
[19] J. Shao, C. Yang, X. Zhu, and X. Lu, The Journal of Physical Chemistry C **114**, 2896 (2010).
[20] J. H. Strange, M. Rahman, and E. G. Smith, Physical Review Letters **71**, 3589 (1993).
[21] K. Lu and Z. H. Jin, Current Opinion in Solid State and Materials Science **5**, 39 (2001).
[22] M. Perez, Scripta Materialia **52**, 709 (2005).
[23] J. B. W. Webber, J. C. Dore, J. H. Strange, R. Anderson, and B. Tohidi, J Phys-Condens Mat **19** (2007).
[24] K. Kaneko, A. Watanabe, T. Iiyama, R. Radhakrishan, and K. E. Gubbins, The Journal of Physical Chemistry B **103**, 7061 (1999).
[25] Q. Jiang, Z. Zhang, and J. C. Li, Chemical Physics Letters **322**, 549 (2000).
[26] R. Kofman, P. Cheyssac, A. Aouaj, Y. Lereah, G. Deutscher, T. Ben-David, J. M. Penisson, and A. Bourret, Surface Science **303**, 231 (1994).
[27] H. Lei, J Phys-Condens Mat **13**, 3023 (2001).
[28] J. Stanek, G. Marest, H. Jaffrezic, and H. Binczycka, Physical Review B **52**, 8414 (1995).
[29] H. J. C. Berendsen, J. P. M. Postma, W. F. van Gunsteren, A. DiNola, and J. R. Haak, The Journal of Chemical Physics **81**, 3684 (1984).
[30] H. Duan, F. Ding, A. Rosén, A. R. Harutyunyan, S. Curtarolo, and K. Bolton, Chemical Physics **333**, 57 (2007).
[31] K. K. Nanda, S. N. Sahu, and S. N. Behera, Physical Review A **66**, 013208 (2002).
[32] H. A. Alarifi, M. Atis, C. Ozdogan, A. Hu, M.Yavuz, Y. Zhou, The Journal of Physical Chemistry C, **117**, 12289 (2013).
[33] E. Marzbanrad, A. Hu, B. Zhao, Y. Zhou, The Journal of Physical Chemistry C, **117,** 16665 (2013).
[34] H. A. Alarifi, M. Atis, C.Özdoğan, A. Hu, M. Yavuz, Y. Zhou, Materials Transactions, **54,** 884 (2013).
[35] Y. Shibuta, Chemical Physics Letters **532**, 84 (2012).

Figure captions

Figure1.(a) Snapshots of Fe_{4800} in nanoconfinements along the axial direction with different Fe-confinement interaction strength ranging from ε=0.1 to 0.8 eV and the insets are the sectional views of the surface at ε=0.4and 0.8 eV which are labeled with M and N respectively; (b) the corresponding total energy per atom as a function of temperature for Fe_{4800} with the interaction strength increasing from ε=0.1 to 0.8 eV. The end of the second slope on the curve was regarded as the melting point of the Fe nanowire.

Figure 2. (a) the surface curvature of the embedded Fe nanowire as a function of the interaction strength when the diameter of confinement range from 16Å to 32 Å; (b)The melting point of the embedded Fe nanowire as a function of the interaction strength when the diameter of confinement range from 16 Å to 32 Å, the inset is the magnitude of the melting point variation between the potential parameter range ε = 0.1-0.8 eV as a function of the diameter; and (c) variation of the melting point as a function of the surface curvature.

Figure 3. Variation of Lindemann indices in the melting process for Fe_{1800} in nanoconfinement (a) at ε=0.1 eV and (b) at ε=0.8eV. In the inserted particle morphology below the Lindemannindices, the green atoms denote the unmelted zones, while the yellow atoms represent the melted zones.

Figure 4. Comparison on the melting pointing between the embedded Fe nanowire and the free Fe cluster with the same curvature. When the surface curvature k = 0.052, the embedded Fe_{4800} and the free cluster Fe_{2500} tend to melt at the same temperature T = 1290 K.

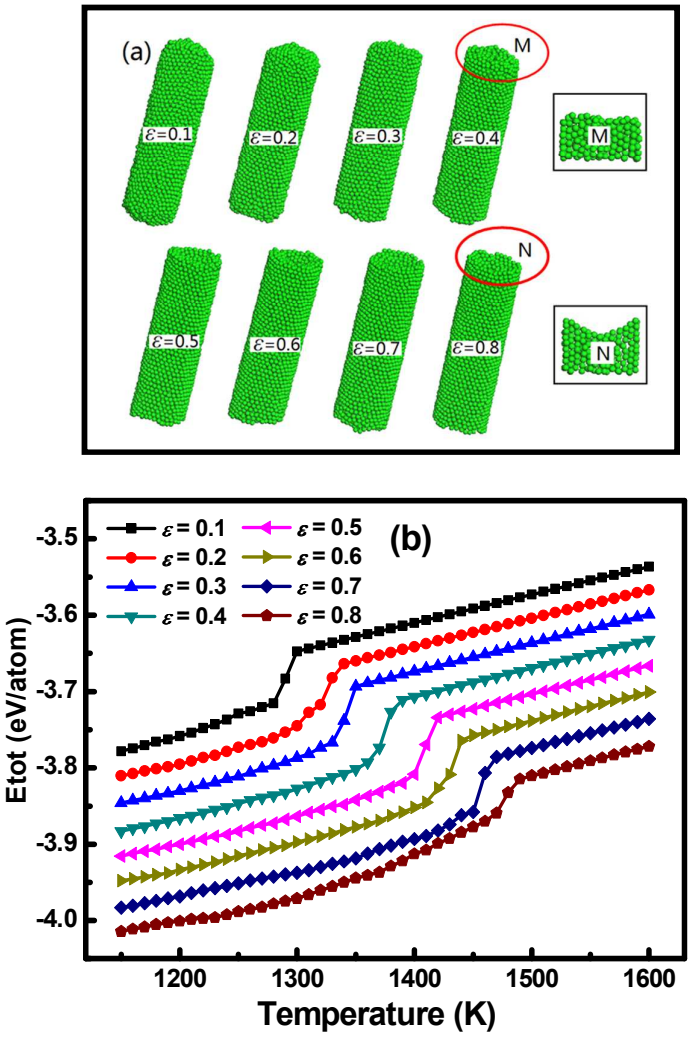

Figure 1

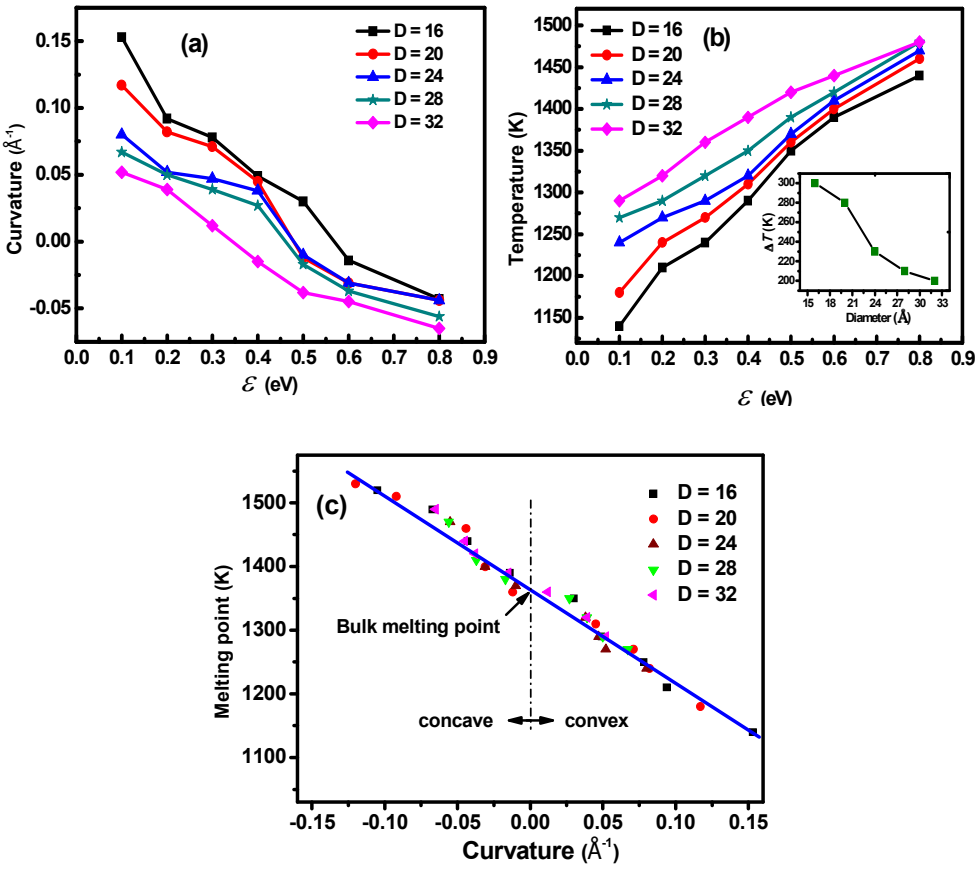

Figure 2.

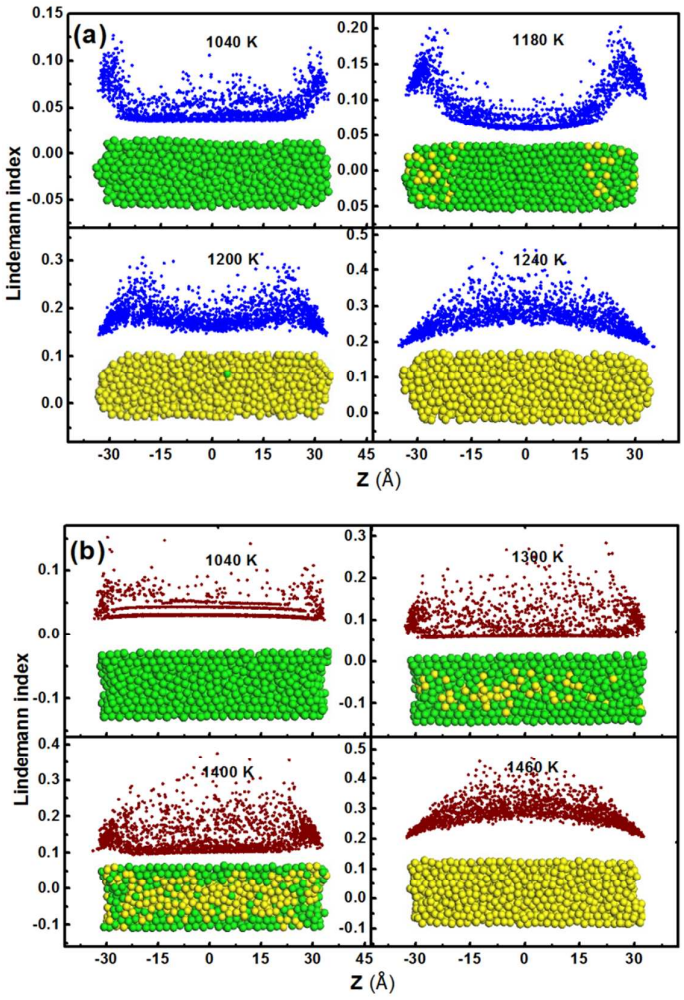

Figure 3.

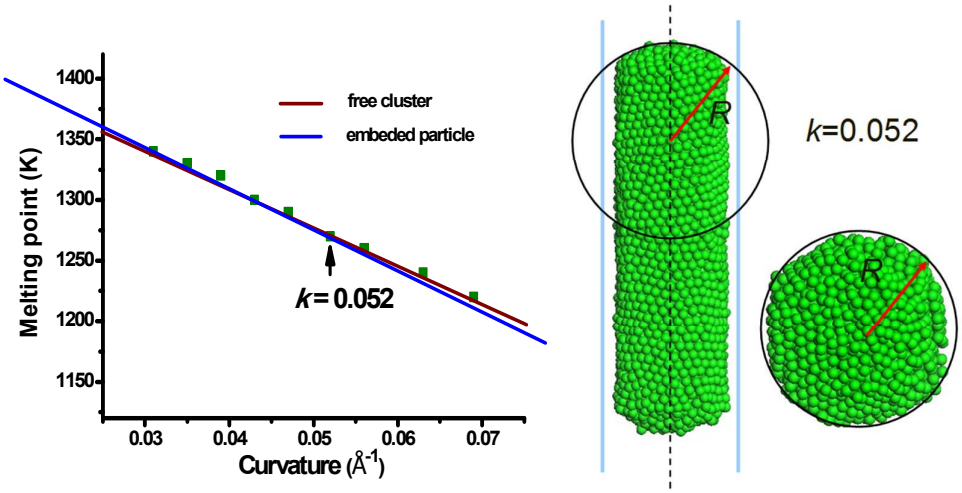

Figure 4.